Fate of Exhaled Droplets From Breathing and Coughing in Supermarket Checkouts and Passenger Cars

Sanika Ravindra Nishandar[1], Yucheng He[1], Marko Princevac[1] and Rufus D Edwards[2]

[1]Department of Mechanical Engineering, Bourns College of Engineering, University of California, Riverside, CA, USA. [2]Department of Epidemiology, Program in Public Health, University of California Irvine, CA, USA.

ABSTRACT: The global pandemic of COVID-19 has highlighted the importance of understanding the role that exhaled droplets play in virus transmission in community settings. Computational Fluid Dynamics (CFD) enables systematic examination of roles the exhaled droplets play in the spread of SARS-CoV-2 in indoor environments. This analysis uses published exhaled droplet size distributions combined with terminal aerosol droplet size based on measured peak concentrations for SARS-CoV-2 RNA in aerosols to simulate exhaled droplet dispersion, evaporation, and deposition in a supermarket checkout area and rideshare car where close proximity with other individuals is common. Using air inlet velocity of 2 m/s in the passenger car and ASHRAE recommendations for ventilation and comfort in the supermarket, simulations demonstrate that exhaled droplets $<20\,\mu m$ that contain the majority of viral RNA evaporated leaving residual droplet nuclei that remain aerosolized in the air. Subsequently ~ 70% of these droplet nuclei deposited in the supermarket and the car with the reminder vented from the space. The maximum surface deposition of droplet nuclei/m^2 for speaking and coughing were 2 and 819, 18 and 1387 for supermarket and car respectively. Approximately 15% of the total exhaled droplets (aerodynamic diameters 20-700 μm) were deposited on surfaces in close proximity to the individual. Due to the non-linear distribution of viral RNA across droplet sizes, however, these larger exhaled droplets that deposit on surfaces have low viral content. Maximum surface deposition of viral RNA was 70 and 1.7×10^3 virions/m^2 for speaking and 2.3×10^4 and 9.3×10^4 virions/m^2 for coughing in the supermarket and car respectively while the initial airborne concentration of viral RNA was 7×10^6 copies per ml. Integrating the droplet size distributions with viral load distributions, this study helps explain the apparent importance of inhalation exposures compared to surface contact observed in the pandemic.

KEYWORDS: SARS-CoV-2, COVID, transmission, decontamination, computational fluid dynamics, aerosols, surfaces, indoor

Introduction

The global pandemic of COVID-19 (caused by the SARS-CoV-2) has highlighted the importance of understanding the transmission dynamics of viruses dispersed in droplets during speaking and coughing. Oral activities such as breathing, talking, and coughing have been shown to emit respiratory droplets carrying infectious virus.[1] The relative importance of exposure pathways through inhalation and contact with surfaces in different community settings is difficult to measure directly but is important due to the prevalence of asymptomatic transmission combined with differences in ventilation, residence time of individuals in different areas, and contact with surfaces across environments. Larger exhaled droplets will settle gravitationally faster than they evaporate, contaminating surfaces in the immediate vicinity of the individual and leading to contact transmission such as a counter top, fabric, or another object,[2] where virus particles may form microscale residues and remain active for extended periods.[3] Smaller droplets are available for direct inhalation or evaporate faster than they can settle and residual virus becomes aerosolized where it may remain entrained in the air for extended periods[4] for subsequent inhalation, impaction on surfaces, or removal by ventilation systems. While the potential for aerosol transmission of respiratory viruses has historically been underestimated,[1,5] the identification of SARS-CoV-2 RNA in aerosols in different areas of 2 Wuhan hospitals during the outbreak of COVID-19 in February and March 2020[6] and the viability of SARS-CoV-2 for hours in particles,[7] combined with widespread case studies of transmission in different environments provide convincing evidence of inhalation transmission. Inhalation doses and surface deposition fluxes for viral genome copies of airborne influenza A viruses indoors at a health center, a day-care center, and on airplanes have also suggested that the aerosol route could be an important mode of influenza transmission while surface deposition was unlikely to produce infectious doses.[8]

Understanding the fate of exhaled droplets, and the balance of transmission pathways in indoor spaces is important in prioritizing risk mitigation approaches and understanding transmission dynamics observed at a population level, particularly as the importance and significance of each transmission pathway may vary in different situations.[5] Lack of quantitative risk assessment of airborne transmission of COVID-19 under practical settings leads to large uncertainties and inconsistencies in preventive measures.[9] Computational studies to understand droplet dispersion in classrooms showed the spread of particles was highly dependent on source location, positioning

of windows, other outlets, and placement of barriers,[10] demonstrating the importance of residence time in evaluating risk through inhalation of airborne nuclei.

This paper simulates the fate of exhaled droplets from coughing and speaking at supermarket checkout counters and in passenger cars as these represent some of the community environments where the potential to contact asymptomatic individuals is enhanced. A range of CFD simulations have been conducted to explore virus transmission in supermarkets and passenger cars, but many of these previous simulations have been hampered by the treatment of the virus-laden droplets as similar to gas diffusion,[11,12] used only 1 or 2 particle droplet sizes, did not account for any evaporation or droplet nuclei deposition[10] or used a range of discrete droplet sizes that don't reflect exhaled droplet distributions.[4,13] Additionally, these studies present modeling frameworks with terminal droplet nuclei sizes that are much larger than those that contain the majority of viral RNA in measured indoor environments.[14,15] Unrealistic treatment of exhaled droplet sizes, the dynamic evaporation in indoor settings, and terminal droplet diameters not only significantly impact the ultimate fate of exhaled droplets containing viral RNA, but also the transport trajectories of these droplets in indoor spaces and the potential for viral transmission. The current simulations advance understanding of transmission in these environments by using measured exhaled droplet size distributions during speaking and coughing and incorporate droplet evaporation combined with realistic terminal droplet sizes based on measured peak concentrations for SARS-CoV-2 RNA in aerosols. Using non-linear distribution of viral RNA across droplet size distributions the current paper explores the resultant time-dependent distribution between airborne droplets and deposition on surfaces, which may help to explain the apparent lower transmissibility for surface contact observed in the pandemic.

Methods

Supermarket checkout counter simulation

The dimensions and layout of the simulated supermarket checkout counter are shown in Supplemental Figure S1, which displays a checkout counter, a shopper, and a vendor inside an enclosure of dimensions $6.5\,m \times 4.3\,m \times 4\,m$. The enclosure consists of 2 fresh air supply inlets ($0.5\,m \times 0.5\,m$) placed on the ceiling and a natural outlet ($2\,m \times 2.5\,m$) on the adjacent wall. Dimensions were approximated from observation of checkout counters in different sized supermarkets in Riverside, California. American Society of Heating, Refrigerating and Air-Conditioning Engineers (ASHRAE) recommends a minimum of 6 to 10 air changes per hour in common retail as well as departmental stores[16] which are subject to change based on occupancy. Fifteen air changes per hour (ACH) were simulated in this scenario. A supply velocity of $2\,m/s$ was calculated based on the ACH requirements as well as specifications for output throw from standard supply diffusers.[16] Based on the

criteria for human comfort recommended by ASHRAE, a temperature of 22°C and relative humidity (RH) of 50% were used in the study.[16] Simulations met ASHRAE standards 62.1 to 2019 using thermal comfort tools (https://comfort.cbe.berkeley.edu/), and as they were on the lower end of the acceptable range would maintain the standard under increased building interior load. The outlet gage pressure was set at zero to reproduce natural outlet ventilation.

Passenger car cabin simulation

The dimensions and layout of the interior of a passenger car based on a Prius, with dimensions $L = 2.5\,m$, $W = 1.5\,m$, and $H = 1.1\,m$ are shown in Supplemental Figure S2 which displays the positioning of 11 fresh air supply vents distributed around the cabin and 3 exhaust vents at the rear of the vehicle. For the simulations presented here, an average supply velocity of $2\,m/s$ was selected based on hot-wire anemometry measurements of air velocity from vents in a car cabin.[17] An ambient temperature of 22°C and relative humidity (RH) of 50% was used in the simulation. The outlet gage pressure was set to zero for the pressure balance of the interior and outside environment. For simplicity, the vehicle is assumed to be moving at a constant speed and all the windows were closed. Opening windows results in rapid ventilation of exhaled droplets, but to our knowledge is not common practice in shared-ride vehicles in Southern California. A mesh with a volume of 600 000 and 300 000 elements was generated in the supermarket checkout area and the car cabin respectively. Meshing parameters and mesh independence study are explained in detail in the Supplemental Information (Supplemental Figures S3 and S4). A no slip boundary condition was applied to all the surfaces in both the cases. Additionally, interior walls, equipment and occupants in the room and sedan car are assumed to be isothermal with the internal temperature and hence no heat loads are modeled in this simulation.

Exhaled droplet emission

This study simulates droplet distributions based on the size of the droplets exhaled while speaking as well as coughing. Additionally, terminal droplet nuclei ($0.3\,\mu m$) which are formed as a result of evaporation of the larger droplets were also simulated. Simulations used exhaled droplet size distributions (1-$700\,\mu m$) for speaking and coughing reported by Chao et al[18], which were measured using Interferometric Mie Imaging (IMI) at a distance of $10\,mm$ from the mouth to minimize evaporation and condensation effects on measured droplet size (see Supplemental Figure S5 for size distributions). The droplets and droplet nuclei are assumed to be passive scalar in these simulations. The droplet distributions used for simulations consisted of 10 sequential coughs during a coughing event and counting from 1 to 10 for the speaking case.[18] A detailed explanation for the calculations on droplet

distributions is provided in the Supplemental Information (Supplemental Tables S1 and S3). Velocities of exhalation through the mouth (30 mm) for speaking and coughing were 3.9 and 11.2 m/s respectively.[18] Exhaled breath was simulated at a relative humidity of 100% and a temperature of 37°C[19]. Once exhaled, droplets rapidly evaporate extending the time larger droplets remain suspended in the air until the droplet reaches a terminal droplet nuclei diameter. Droplet evaporation depends on the equilibrium vapor pressure on the droplet surface relative to the partial pressure of water vapor in the ambient air which is controlled by the droplets specific area and ambient conditions including the air temperature, relative humidity, turbulence, and the solute concentration.[20] Over the time frame of the current simulations droplet evaporation rates were not overly impacted by water compared to saliva.[20] In these simulations, a terminal droplet nuclei diameter of 0.3 μm was used, rather than estimating solute concentrations, because the largest sub-micrometer peak concentration of SARS-CoV-2 RNA measured in aerosols in 2 Wuhan hospitals during the outbreak of COVID-19 in February and March 2020 falls in the middle of the aerosol size range of 0.25 to 0.5 μm[6]. Terminal droplet nuclei allow multiple viral particles in a single droplet since virions of SARS-CoV-2 have been characterized to be in the range of 70 to 100 nm.[21,22] In addition, 0.3 μm allows for a worst-case evaluation of filtration approaches as this is the most penetrating particle size for N95 respiratory masks and corresponds to MERV (Minimum Efficiency Reporting Value) criteria for HVAC (Heating, Ventilation, and Air Conditioning) filter media which can vary within a range of 150 to 500 nm depending on particles' shape, charge, or relative humidity.[23]

Droplet dynamics and evolution

To delineate relevant droplet behavior in given indoor flows, computational fluid dynamics (CFD) simulations were performed using Ansys® Academic Research Fluent, Release 19. Trajectory and tracking of the individual particles are done using a coupled Euler-Lagrange approach in the Discrete Phase Model (DPM) module. In this approach, the fluid phase is computed using Reynolds-averaged Navier Stokes (RANS) using the K-ε turbulence model. Since we are studying the trajectories of droplets in indoor space, the K-ε model is well suited as it is better at predicting fully developed flows away from the walls than the K-ω model, which accurately predicts near-wall interactions and is more suitable for strongly boundary layer dominated flows inside turbomachinery applications. Exhaled droplets from coughing and sneezing are modeled as liquid droplet particles that obey conservation of momentum as well as heat exchange by associating the sensible heat flux in the droplet with the convective and latent heat transfer between the droplet and the fluid phase. The conservation of momentum on a droplet is given by:

$$\frac{du_p}{dt} = F_D\left(u - u_p\right) + \frac{g\left(\rho_p - \rho\right)}{\rho_p} + F \qquad (1)$$

where, F_D, u, u_p are the drag force per unit particle mass, fluid velocity, and particle velocity respectively. The second term includes gravitational acceleration (g), particle density (ρ_p) and fluid density (ρ). F constitutes all the additional forces such as Thermophoretic Force, Brownian Force, and forces that arise due to rotation of the reference frame.

Positive molar flux results in evaporation and reduction in particle size after they are expelled from the mouth. The rate of vaporization was governed by:

$$N_i = k_c(C_{i,s} - C_{i,\infty}) \qquad (2)$$

where, N_i is the molar flux, k_c is the mass transfer coefficient, $C_{i,s}$ is the vapor concentration at the droplet surface and $C_{i,\infty}$ is the vapor concentration in the bulk gas. Since evaporation of droplets is rapid, coagulation of the droplets was not simulated. Boundary conditions for all surfaces were set to trap liquid droplets, which in terms of the DPM simulation implies that the trajectory calculations are either terminated at the surface or when droplets evaporate. More details on modeling parameters are provided in Supplemental Information.

Viral load in droplets and droplet nuclei

Average viral load for SARS-CoV-2 in the sputum was reported to be 7.00×10^6 copies per ml.[24] Viral RNA is distributed in droplets based on their site of origin[25] where 85.4% of the total exhaled RNA come from fine droplets (≤5 μm) generated deeper in the respiratory tract where there are high levels of viral shedding.[26] Viral load within each exhaled droplet size bin was apportioned 85% viral load in droplets with diameters less than 10 μm, 10% in the droplets 10 to 20 μm, and 5% in the droplets 20 to 100 μm where viral RNA within each size bin was distributed equally across the size dependent number fraction of exhaled droplets. The number of virions deposited on surfaces was estimated based on the number of droplets impacting on each surface after evaporation and transport in the room and viral load of the corresponding droplet at the point of exhalation. To evaluate the sensitivity of the viral concentrations on surfaces to distributional assumptions, Supplemental Figures S7 and S8 show the allocation of viral RNA based on the volume distribution of droplets within each size bin.

Results
Supermarket checkout counter simulation

The trajectories and ultimate fate of exhaled droplets in supermarkets and passenger cars are dependent on droplet size, solute concentration, initial droplet velocity, temperature, as well
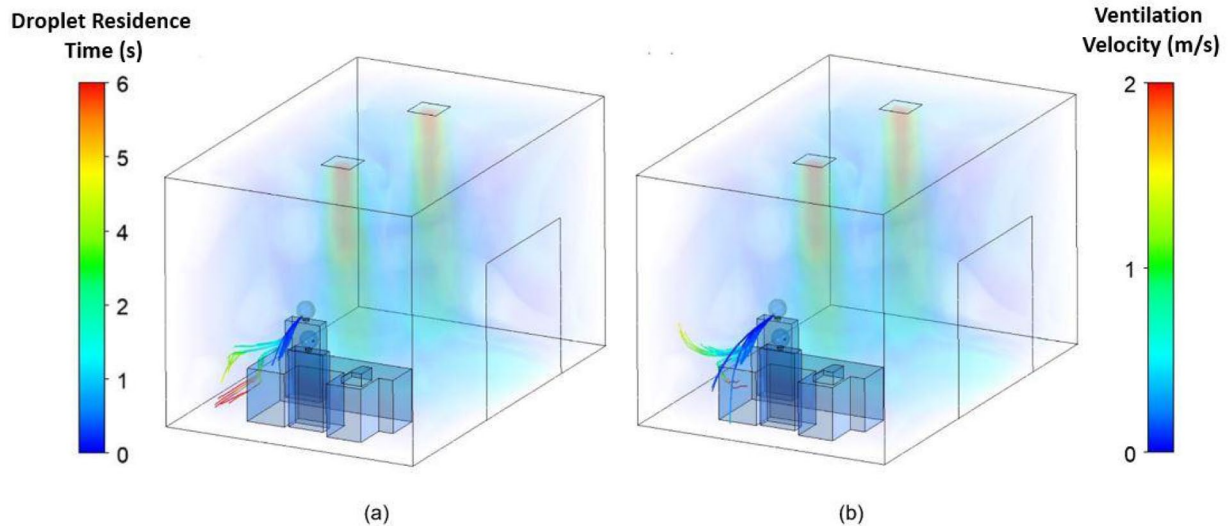
Figure 1. Droplet trajectories and deposition in a simulated supermarket checkout area with ventilation velocity of 3 m/s after: (a) continuous speaking with an initial flow velocity of 2 m/s and (b) coughing with an initial flow velocity of 11.2 m/s. Droplet trajectories are solid lines emitted from the occupant. Ventilation velocities are background coloration inside the space.
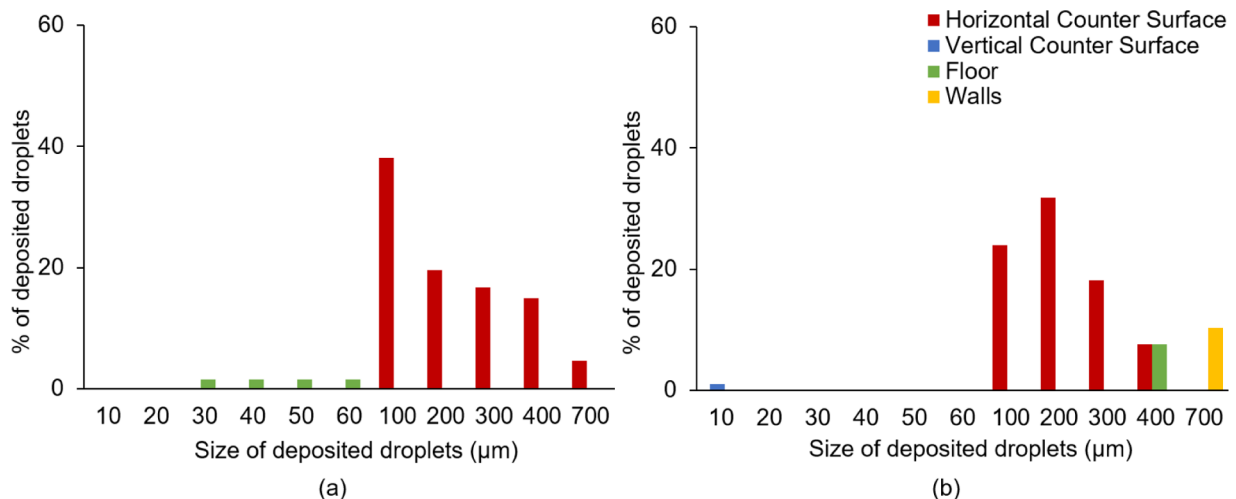

Figure 2. Droplet size distribution at the point of deposition and location of deposition for exhaled droplets around the supermarket checkout counter after: (a) speaking and (b) coughing.

as relative humidity. Additionally, air circulation patterns due to ventilation are critical to understanding the trajectory of droplets in indoor spaces. Figure 1 shows droplet trajectories around a supermarket checkout counter during (a) speaking and (b) coughing where the color scale on droplet trajectories represents the residence time of droplets in the air. Air velocity as a result of ventilation is reflected in the color contours in the interior space. Fresh air enters the room at the top where maximum velocity regions can be seen. As the momentum of the droplets emitted during speaking is much less than during a cough, the particles deposit closer to the individual compared to coughing. Recirculation zones near the floor and in proximity to the counter formed due to complexity in geometry can trap the droplets and result in deposition in these areas.

Figure 2a and b depict the size distribution of the droplets at the point of deposition, on surfaces around the checkout counter while speaking and coughing, respectively. The diameters of majority of the droplets that deposited on the counter surface were in the range of 100 to 700 μm in both cases. After speaking, large droplets in the range of 400 to 700 μm were airborne for a short time and deposited on the nearby counter surface due to the effect of gravity. Droplets with an intermediate size range of 100 to 400 μm were also deposited on the counter surface as an effect of the low release velocity while speaking combined with gravitational influences. Small droplets in the range of 30 to 100 μm get equally affected by gravity as well as the drag force, which enables them to get carried by the airstream and deposit on the floor farther from the counter. Droplets smaller than ~20 μm evaporate in a short time and hence there is no initial deposition observed in this size range. After coughing, however, the higher release velocity and inertia of the droplets larger than 300 μm enable them to travel farther
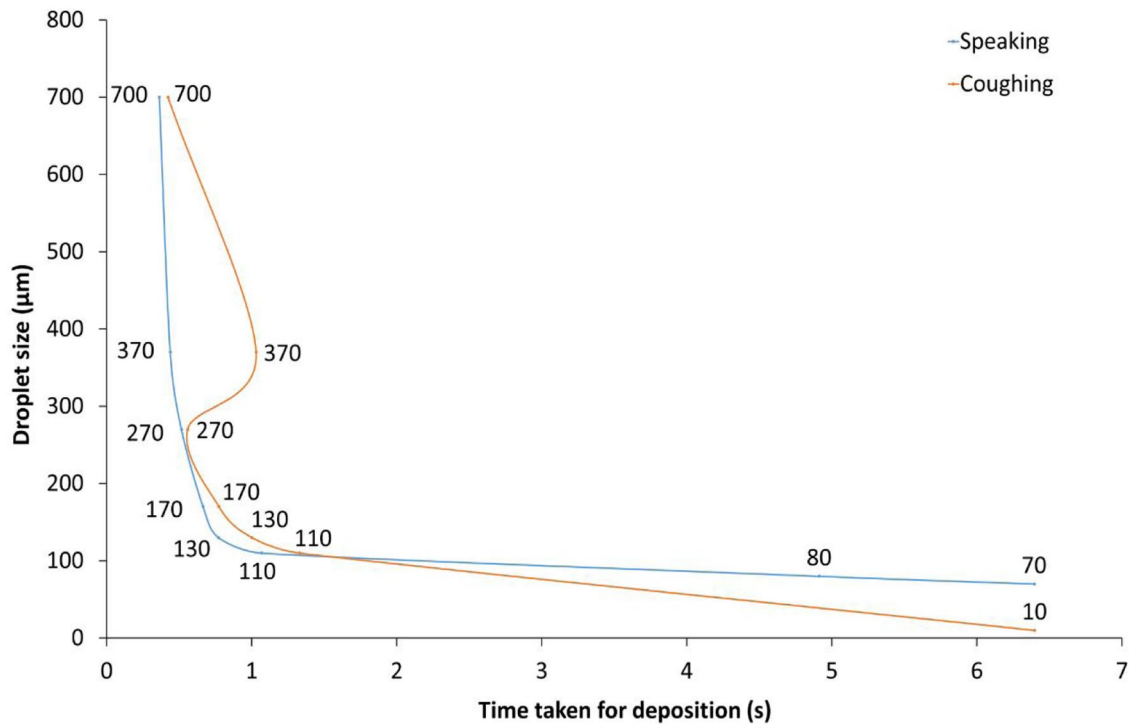
Figure 3. Time taken by different sized droplets to deposit on the surfaces in the supermarket. Data labels indicate approximate diameters of the deposited droplets.

and deposit on the wall. The particles in the range of 100 to 300 μm deposit on the counter surface similar to droplets emitted after speaking. No initial particle deposition in the range of 30 to 100 μm was observed in this case.

Figure 3 shows the time taken for exhaled droplets to deposit on surfaces based on their diameters. In both the scenarios, speaking as well as coughing, droplets in the range of 100 to 700 μm, deposit on nearby surfaces in under a second after emission. Droplets with diameters in the range of 10 to 100 μm deposit at a farther distance with deposition largely ending after ~6 seconds. The increased time for droplets 369 μm to deposit relative to 271 μm droplets after coughing is due to the projection of these droplets beyond the counter surface for subsequent deposition on the floor. The maximum concentration of deposited droplets as a result of counting 1 to 10 was 15 droplets/m². Whereas the maximum concentration as a result of coughing 10 times was 478 droplets/m². The average surface concentrations for speaking and coughing were 1 and 26 droplets/m², respectively. Exhaled droplets < ~20 μm that evaporate rapidly and remain suspended in the air as residual droplet nuclei (0.3 μm) constitute ~85% of exhaled droplets and remain entrained in the air until they are either deposited on farther surfaces or are flushed out by the ventilation system.

Figure 4 shows the trajectory of droplet nuclei with a terminal droplet diameter of 0.3 μm, which due to their small inertia, follow the path of ventilated air. Of these entrained droplet nuclei ~70% remain suspended in the air till they are ventilated from the space after 225 seconds based on 15 ACH, while the remainder deposit at low concentration on other surfaces in the room. The average lifetime of aerosolized droplet nuclei in the supermarket simulation was much shorter than the half-life for SARS-CoV-2 viability in the air.[7] Average surface concentrations of 107 droplet nuclei/m² were deposited in the room under the coughing scenario with a maximum surface concentration of 819 droplet nuclei/m² in the vicinity of the checkout counter. Average surface concentrations of 2 droplet nuclei/m² were deposited in the room during speaking with a maximum surface concentration of 3 droplet nuclei/m² in the vicinity of the checkout counter.

Passenger car cabin simulation

Figure 5 shows the contours of the flow field velocity, determined by the ventilation system and the cabin geometry, along with droplet trajectories and deposition on surfaces during (a) speaking and (b) coughing in a passenger car. Air enters the domain through 11 vents distributed on the front dashboard, where the maximum velocity magnitude region is located. The trajectories of the droplets are dependent on initial speaking and coughing velocities as well as the flow field inside the cabin, with almost all droplets reaching the front dashboard after coughing, while lower velocities from speaking result in deposition of intermediate size droplets on the human body and the floor. Since droplet trajectories are dependent on the airflow inside of the sedan cabin generated by the air-conditioning system, changes in ventilation strength and direction would affect deposition patterns.
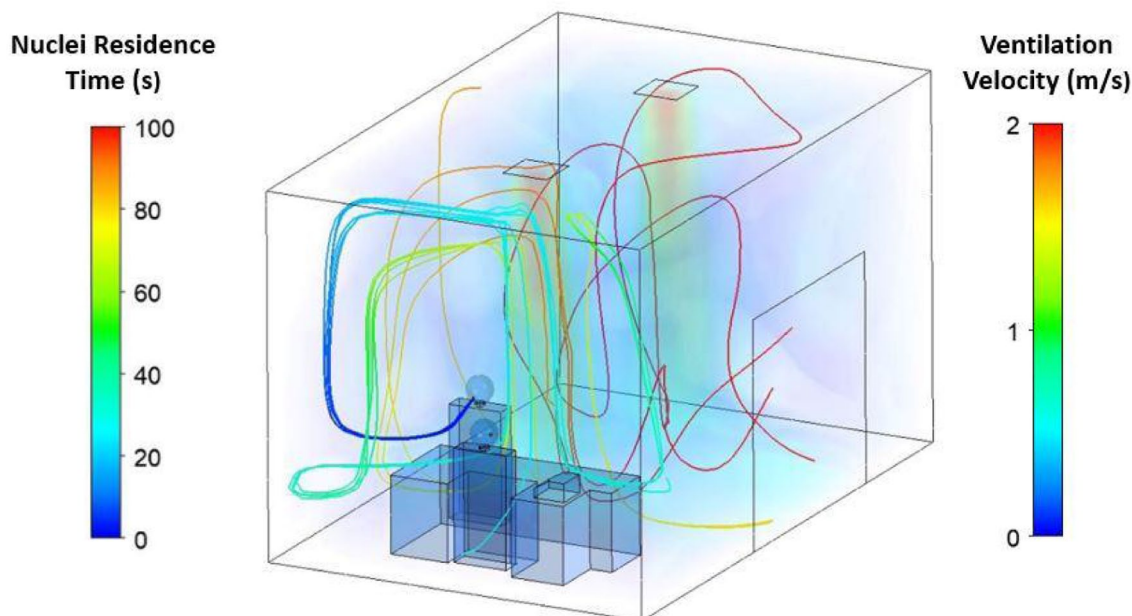
Figure 4. Droplet nuclei trajectories in a simulated supermarket checkout area after droplet evaporation.
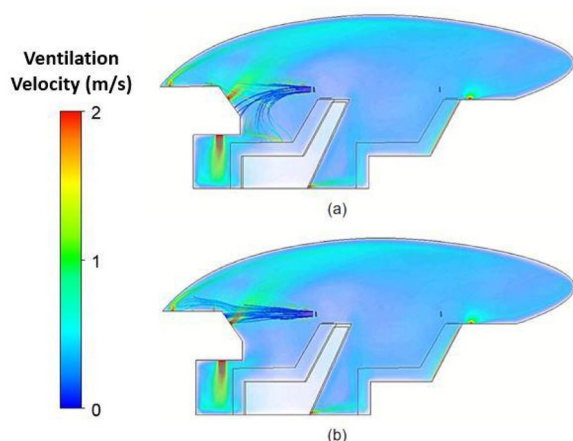

Figure 5. Exhaled droplet trajectories in the air and deposition on surfaces during speaking and coughing in a passenger car: (a) speaking and (b) coughing.

Figure 6 shows the droplet deposition on surfaces after speaking and coughing which is influenced by the combination of drag force, gravity, and other forces including inertia, which impacts droplet sizes to a different extent. Due to the high release velocity of 11.2 m/s during coughing, droplet displacement is dominated by inertia, and droplets travel directly forward to deposit on the front dashboard as shown in Figure 6b. Average concentrations of 59 exhaled droplets/m² were simulated from coughing with a maximum surface concentration of 139 exhaled droplets/m² on the front dashboard. Lower release velocities during speaking (Figure 6a), resulted in the deposition of smaller droplets (10-60 µm), which are dominated by drag, on the front dashboard. Intermediate sized droplets (60-160 µm), which are more impacted by gravitational forces, deposit on the floor and the human body, and larger droplets (270-750 µm), which are dominated by inertia, deposit on the front dashboard. Average surface concentrations of 76 exhaled droplets/m² were simulated after speaking, with a maximum surface concentration of 89 exhaled droplets/m² on the front dashboard.

Figure 7 shows the relative deposition of droplets on surfaces and entrainment of aerosolized droplet nuclei in the interior space of the car over time. Droplets with an initial droplet diameter $<$ ~20 µm evaporate and remain suspended in the air as residual droplet nuclei which are transported through the domain by ventilation before exiting the domain. Due to the smaller domain and proximity of surfaces, exhaled droplet deposition occurs within ~1.4 second. However, even in this scenario the droplets in the range 700 to 200 µm deposit in a short time while the droplets in the range 20 to 200 µm deposit more gradually.

Figure 8 shows trajectories for the evaporated droplet nuclei that remain suspended in the air. The movement of the droplet nuclei follows the ventilation air flow field in the car, which is independent of the initial droplet release condition. Thus, the trajectory of nuclei after both speaking and coughing remains the same. However, surface concentrations vary based on different numbers of exhaled droplets during speaking and coughing. Average surface concentrations of 187 droplet nuclei/m² were simulated after coughing, with a maximum surface concentration of 1387 droplet nuclei/m² on the front dashboard. Average surface concentrations of 5 droplet nuclei/m²were simulated after speaking, with a maximum surface concentration of 18 droplet nuclei/m² on the front dashboard. Although, changes in ventilation settings play a greater role in whether these droplet nuclei contact surfaces to deposit.
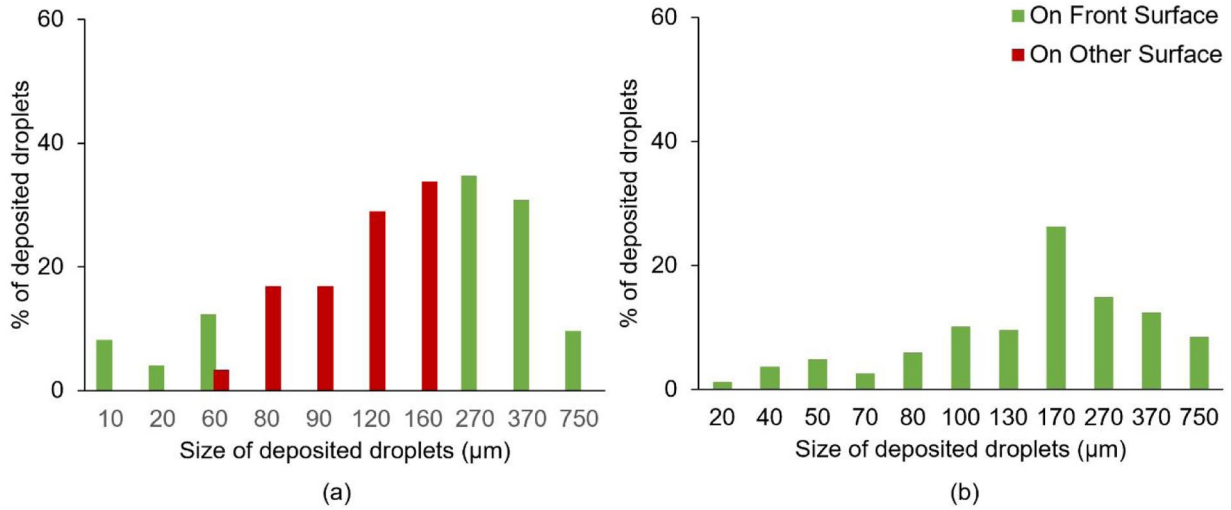
Figure 6. Droplet size distribution at the point of deposition and location of deposition in passenger car after: (a) speaking and (b) coughing.
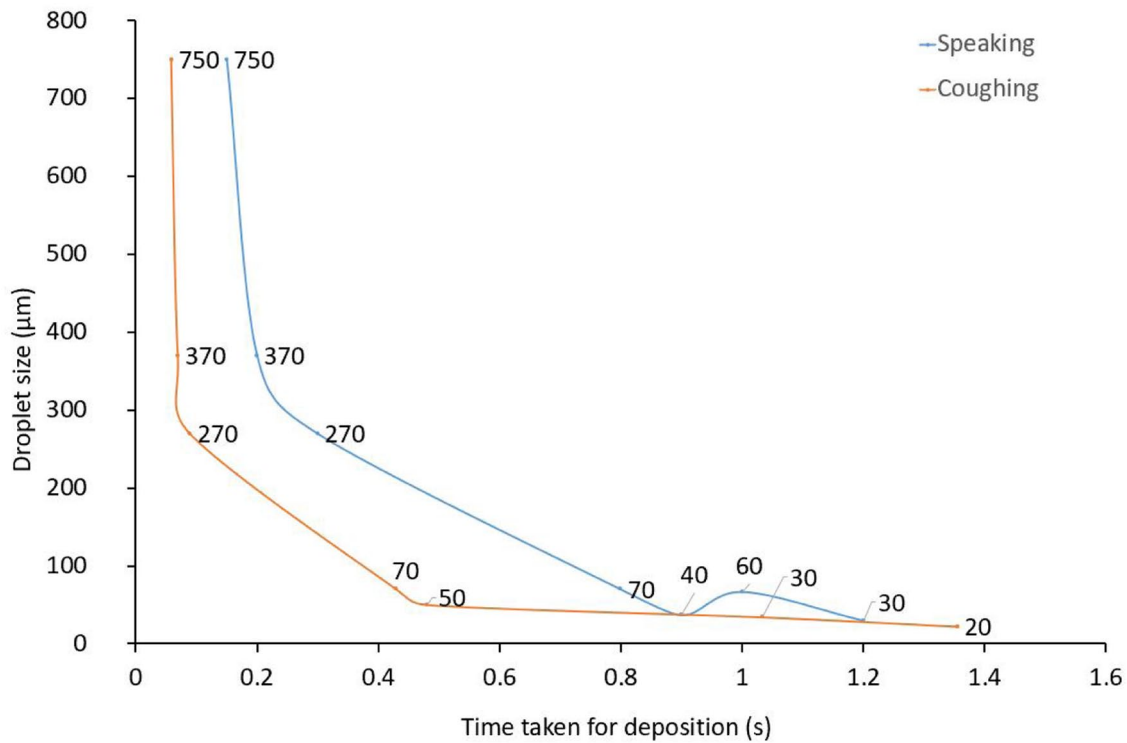
Figure 7. Time taken by different sized droplets to deposit on the surfaces in the sedan cabin. Data labels indicate approximate diameters of the deposited droplets.
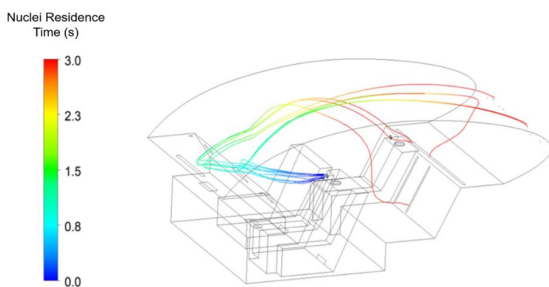
Figure 8. Exhaled droplet nuclei trajectories inside the passenger car.

Discussion

The simulations of passenger cars and supermarkets presented here are the only ones, to our knowledge, that combine published exhaled droplet size distributions during speaking and coughing, with realistic terminal droplet sizes based on measured indoor peak concentrations for SARS-CoV-2 RNA in aerosols. The objective of these simulations was to simulate both the fate and deposition of exhaled droplets, and also the subsequent fate and deposition of aerosolized droplet nuclei to examine both the potential for aerosolized transmission of

SARS-CoV-2 RNA, and also the ultimate fate of the exhaled droplets in deposition on surfaces. A range of other CFD simulations have been conducted to explore virus transmission in supermarkets and passenger cars, but many of these simulations have been hampered by unrealistic treatment of exhaled droplet size distributions, the dynamic evaporation of droplets present in indoor settings, and the resultant terminal droplet nuclei diameters, which significantly impacts the ultimate fate of exhaled droplets containing viral RNA, the transport trajectories in indoor spaces, and thus the potential for viral transmission.

Simulations in supermarkets include 2 discrete particle sizes of 5 and 20 μm with contact surfaces having different particle attachment efficiencies,[15] but do not take into account the size distribution of exhaled droplets as well as the evaporation of droplets after emission. Similarly, identifying high-risk areas in a grocery store based on infected individuals along a defined route and emitting viral aerosols in the range of 0.3 to 3 μm[27] also did not incorporate size distributions of exhaled droplets as well as the evaporation of droplets after emission. Simulations in passenger car cabins estimate the risk of infection from SARS-CoV-2 Delta variant during breathing and speaking in the presence of different ventilation modes[28] used particle sizes between 2.4 and 90 μm with an assumption that the droplets evaporate as soon as they are emitted. However, in the simulations presented here trajectories of exhaled droplets differ from those of residual droplet nuclei as a result of size-dependent competing forces.

Simulations in other indoor environments assumed all droplets evaporate immediately after expulsion from the oral cavity and treated virus-laden droplets as similar to gas diffusion to quantify the exposure to fine droplet nuclei at each table in a poorly ventilated restaurant,[12] and in indoor classrooms,[11] validated with tracer gas measurements. Other simulations have used only 1 or 2 particle droplet sizes that don't reflect exhaled droplet distributions and do not account for any evaporation or droplet nuclei deposition,[29] or assume immediate evaporation of droplets and simulate 6 discrete size bins (1, 4, 10, 15, 20, and 50 μm) for particles in the range of 1 to 50 μm to examine aerosol transport and deposition of particles in a classroom in the presence of glass barriers,[10] and to assess different intervention strategies to reduce infection for multiple passenger capacities in a Boing 737 aircraft cabin.[30] Assuming immediate evaporation of droplets, however, doesn't consider the initial release trajectory of exhaled droplets and subsequent transport trajectories in indoor spaces. Another framework developed for COVID simulation in indoor environments[31] does not incorporate evaporation and uses a terminal droplet nuclei size of 12.5 μm which is much larger than particle sizes shown to contain the majority of viral RNA measured in indoor aerosols,[6] which would tend to overestimate the amount of deposition, change deposition locations and underestimate residence time in the air. Although particles <5 μm were

estimated to be negligible for infection risk, SARS-COV2 RNA in indoor aerosols is most prevalent in this size range.

Deposition of viral RNA

The majority of droplets emitted during speaking and coughing in these simulations of supermarket checkout and passenger car cabins evaporated leaving residual aerosolized droplet nuclei that have been suggested to be an important component of apparent airborne transmission of SARS-CoV-2.[25,32-34] Similar evaporation of smaller droplets has been reported theoretically,[35] from physical measurement[36] and models based on chemical kinetics.[37] In general, evaporation of exhaled droplets was favored for droplets with an initial size <20 μm in diameter and larger initial droplet diameters 20 to 700 μm settled on surfaces suggesting the potential for virion transmission from larger droplets on surfaces. Viral RNA, however, is not uniformly distributed across exhaled droplet size distributions and droplet counts are not direct predictors of viral load. Several experimental studies have been conducted since the onset of the SARS-COV-2 pandemic to quantify the viral load exhaled as a result of oral activities which include speaking, coughing, breathing, and singing. A median of 713.6, 447.9, and 63.5 N gene copies exhaled while singing, talking, and breathing respectively resulted in fine aerosols (≤5 μm) contributing 85% of the total viral load.[26] Similarly, high concentrations of SARS-CoV-2 RNA were measured in aerosol distributions in hospitals in Wuhan that showed peak concentrations of 40 and 9 copies m^{-3} in the 0.25 to 0.5 μm and 0.5 to 1.0 μm range, respectively, and concentrations of 7 copies m^{-3} in droplets >2.5 μm[6]. Further, active replications of virions were observed in particles <1 μm, with some evidence in particles <4 μm.[38] Viral load in the sputum for a combination of symptomatic and asymptomatic subjects generally ranged between 10^4 and 10^{11} copies per ml.[39-42] In general, viral RNA is distributed in droplets based on their site of origin.[25] Viral load is distributed predominantly in smaller aerosols, and can be attributed to the generation of small droplets in regions where there are high levels of viral shedding deeper in the respiratory tract, although the amount of shedding varies largely between individuals.[43] During talking and singing, the fine droplet (≤5 μm) fraction contain 85.4% of the total exhaled RNA.[26] In contrast, droplets in the size range 10-700 μm which are produced in the larynx and oral cavity respectively, contain smaller fraction of the viral load.[44] Viral content for current CFD simulations assumed an average viral load of 7.00×10^6 copies per ml in the sputum,[45] apportioned 85% viral load in droplets with diameters less than 5 μm, 10% in the droplets 10 to 20 μm, and 5% in the droplets 30 to 700 μm where viral RNA within each size bin was distributed equally across the size dependent number fraction of exhaled droplets.
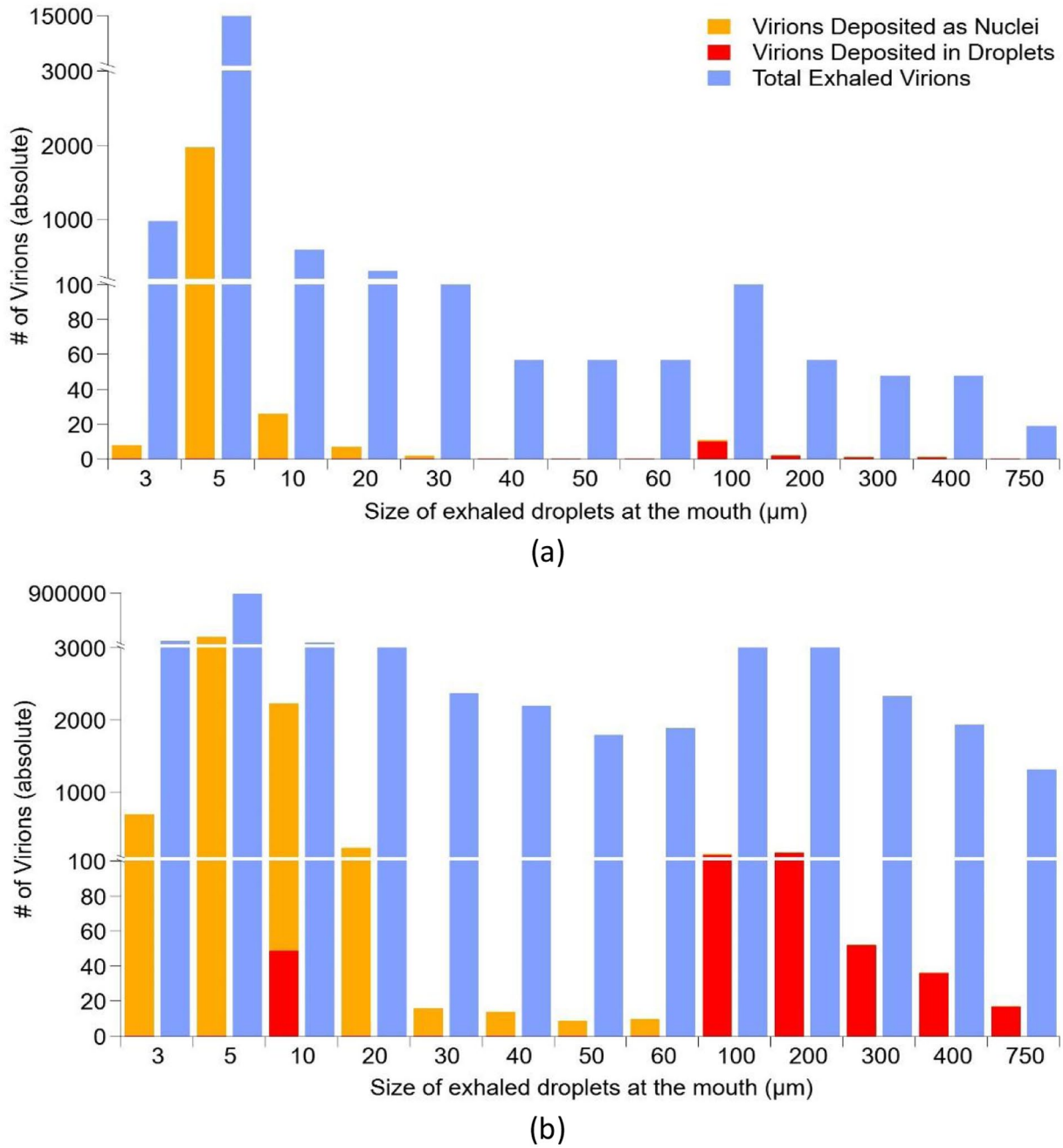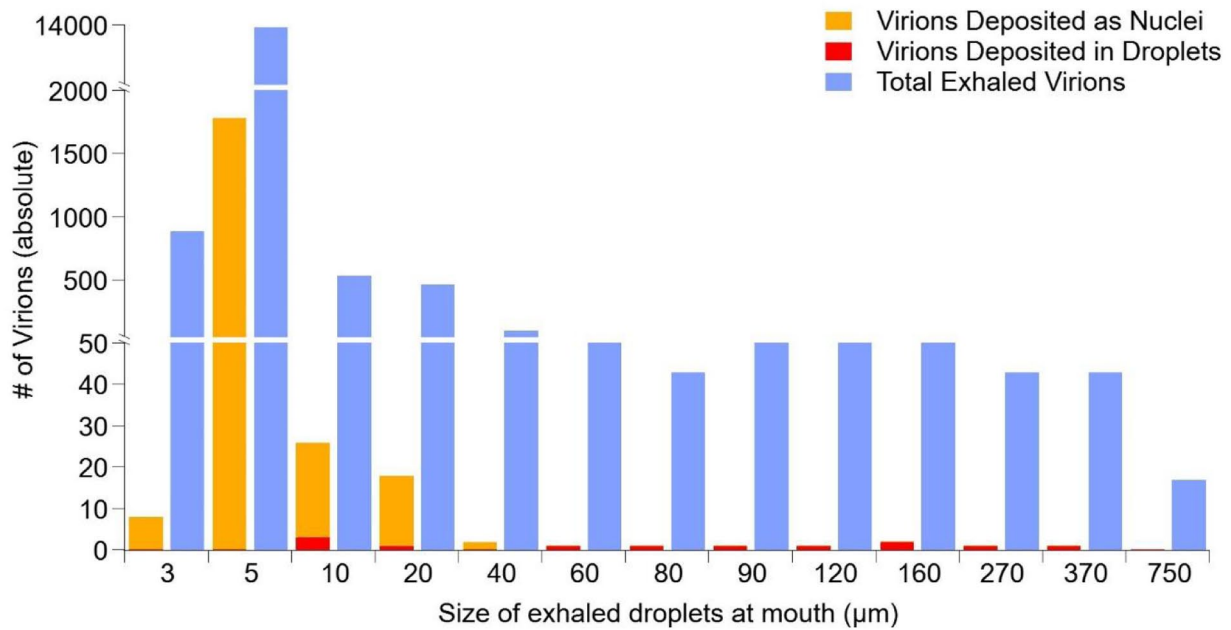
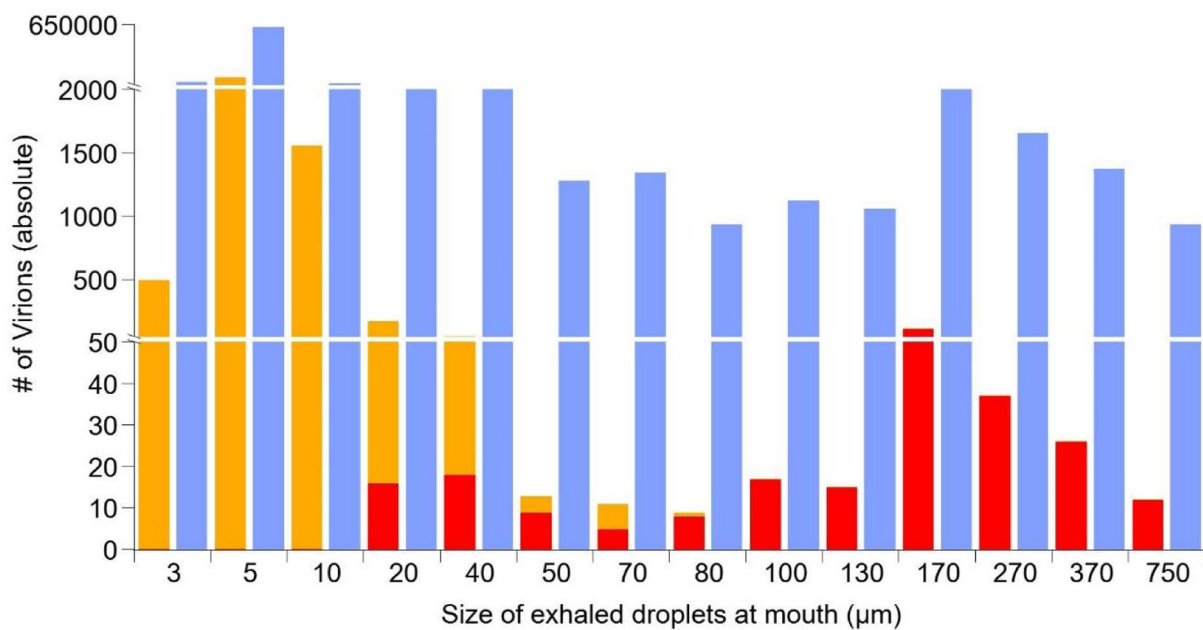**Figure 9.** Deposition of viral RNA on surfaces in the supermarket after: (a) speaking and (b) coughing.

Figure 9 shows the numbers of virions in exhaled droplets and droplet nuclei that deposited on surfaces in the supermarket. Approximately 11% and 13% of exhaled virions deposited on surfaces in the supermarket after speaking and coughing respectively, with 0.1% in both cases depositing in the checkout area and the remainder on surfaces further away in the room. Of the 11% of total exhaled virions that deposited on surfaces after speaking about 10.5% originated from exhaled droplets <10 µm, 0.4% from droplets 10 to 20 µm, and 0.1% from droplets greater than 20 µm, respectively. Similarly, of the 13% of total exhaled virions that deposited on surfaces after coughing approximately 12% originated from exhaled droplets <10 µm, 0.5% from droplets 10 to 20 µm, and 0.1% from droplets greater

than 20 µm, respectively. For both speaking and coughing, the vast majority of exhaled virions (89% and 87% for speaking and coughing respectively) remained entrained in the air until they were ventilated out of the space. Maximum and average viral RNA obtained on surfaces in the supermarket were 70 and 45 virions/m² for speaking and 2.3×10^4 and 3×10^3 virions/ m² for coughing, respectively.

Figure 10 shows the numbers of virions in exhaled droplets and droplet nuclei that deposited on surfaces in the passenger car cabin. Approximately 11% and 13% of exhaled virions deposited on surfaces in the passenger car cabin after speaking and coughing respectively, with 0.1% in both cases depositing in front dashboard and the remainder on surfaces further away

(a)

(b)

Figure 10. Deposition of viral RNA on surfaces in the passenger car after: (a) speaking and (b) coughing.

in the car cabin. Of the 11% of total exhaled virions that deposited on surfaces after speaking approximately 10.5% originated from exhaled droplets <10 μm, 0.4% from droplets 10 to 20 μm, and 0.1% from droplets greater than 20 μm, respectively. Similarly, of the 13% of total exhaled virions that deposited on surfaces after coughing approximately 12% originated from exhaled droplets <10 μm, 0.5% from droplets 10 to 20 μm, and 0.1% from droplets greater than 20 μm, respectively. For both speaking and coughing, the vast majority of exhaled virions (89% and 87% for speaking and coughing respectively) remained entrained in the air until they were

ventilated out of the space. Maximum and average viral RNA on surfaces in the passenger car were 1.7×10^3 and 238 virions/m² for speaking and 9.3×10^4 and 1.2×10^4 virions/m² for coughing, respectively.

In the current simulations exhaled droplets <20 μm evaporated resulting in aerosolized droplet nuclei which contain the majority of the viral load that remain entrained in the air, highlighting the importance of the inhalation exposure pathway in the short time after emission. While some of these residual droplet nuclei were deposited on interior surfaces (walls and floor) further away from the individual, deposition

concentrations were low. Larger droplets (20-700 μm) deposit on surfaces in the vicinity of the carrier, but have low viral loads based on reported distributions of viral RNA across droplet sizes, which may help to explain the apparent lower transmissibility for surface contact observed in the pandemic.

While these simulations are instrumental in tracking the fate of exhaled droplets that contain the majority of the exhaled viral load, the link between exhaled viral loads and the risk of infection is more complex. Although generally accepted that the probability of becoming infected indoors will depend on the total amount of SARS-CoV-2 emitted from an infected individual and subsequently inhaled,[2] the transmission of respiratory viruses is dependent on a range of other virus-host relationships which make direct relationships between models of aerosol transmission of virus-laden droplets and infection in individuals more complex.[8] For example, controlled studies of aerosol transmission of SARS-CoV-2 and seasonal H1N1 influenza viruses between ferrets were dependent on viral strain, the degree of mucosal inflammation which attenuated viable exhaled virus, and viral replication efficiency. Further, although exhaled viral RNA remained constant, transmission efficiency diminished from day 1 to day 5 after donor infection.[46] In humans, infection with SARS-CoV-2 in most people typically produces either mild or no symptoms of COVID-19 because the innate and adaptive immune responses can rapidly eliminate the virus, and severe disease with hospitalization occurs only when such immune responses are delayed or inadequate.[47,48] As a result, the number of virions required for an infectious dose is not currently known and based on individual's immune responses and air conditioning in nasal passages[49] will vary among individuals.

Other factors influencing viral transmission

Droplet trajectories and the relative proportions depositing or exiting the domain varied significantly between speaking and coughing as the velocity of the incoming air from vents in both the supermarket and the passenger car impacts droplet trajectories. Further, faceted droplets formed by the presence of salt residues from lung fluid of the lower respiratory tract have been reported,[9,50,51] which may alter deposition characteristics in respiratory passages. In general, droplet trajectories are more impacted during speaking than coughing as they are emitted with a lower velocity. These low-velocity droplets are less likely to impact on surfaces directly in front of the individual and are more likely to evaporate leaving droplet nuclei. During coughing, droplets are emitted with larger inertia which results in greater deposition on surfaces immediately in front of the individual. Although there is a range of speaking and vocal activities not represented in droplet size distributions reported by Chao et al,[18] which would result in different trajectories and deposition characteristics, speaking and coughing are thought

to be important in the dissemination of viral particles in droplets from the mouth. Evidence of viral transmission from singing in superspreading events,[52] however, demonstrates that other activities and superspreading events play important roles in viral transmission.[53]

Velocities of exhaled droplets, as well as particle distributions, vary between individuals, and subsequent size reduction through evaporation is dependent on solute concentrations and environmental conditions. Simulations in the supermarket used ASHRAE criteria for human comfort as a basis for simulations (15 ACH, Temperature 20°C, Relative Humidity 50%), as these guide HVAC operation in commercial spaces. Significant deviation from ASHRAE criteria for human comfort in smaller supermarket venues for energy conservation would result in longer residence time of aerosolized droplet nuclei. Increasing the ACH rates by 5 reduces the droplet nuclei residence time by 20 seconds in the supermarket in these simulations, and significantly greater changes in ventilation rates would be required to reduce the potential for inhalation exposure, with concurrent increases in energy costs. Simulations of supermarket counters using a different orientation for the outlet did not show substantial differences in the trajectory, surface deposition as well as the rate of evaporation of the droplets (Supplemental Figure S6). Although the orientation of the outlet did not result in major differences in surface deposition, the complexity of the domain, including the position of fresh air supply inlets, shelve orientation, and heights may play a role in creating dead spaces that increase residence time and droplet deposition in these areas. Barriers in a classroom reduced the numbers of aerosolized droplets due to increased deposition on the barrier surface, but the barrier also obstructed the removal of droplets from the indoor environment by ventilation.[10] Interior walls, equipment and occupants in the room are assumed to be isothermal with the room temperature and hence no heat loads are modeled in this simulation. Incorporating radiation induced heat loads may vary the ventilation flow field in the indoor environment. Finally, automatic opening and shutting of entrance doors to allow entry of customers and for energy conservation is common in supermarkets, which may result in some backflow as warm air enters. In these simulations the door of the supermarket remained open, as automatic doors could not be integrated with these models, as air curtains on automatic doors minimize the degree of backflow into interior spaces.

In the passenger car temperature and RH are inherently more variable due to windows and doors but passenger comfort ranges still imply temperatures of approximately 26°C and RH 55%.[54] Clearly, however, scenarios where the temperature and RH are widely different from these values could result in different patterns of droplet aerosolization and deposition. Droplet deposition and trajectories in the passenger car are also dependent on velocity and directional flow from air supply vents. Directional vents combined with programmable venting

modes and individual vent closures reflecting user preferences can significantly impact droplet trajectories. In current simulations, the vents are open and positioned to direct airflow directly to the driver, with windows closed, which is most commonly used to reduce buffeting and noise in the cabin. In contrast to the supermarket scenario, speaking by the driver in the passenger car results in a greater relative fraction of deposited droplets on surfaces as the ventilation directly toward the driver results tends to recirculate the droplets toward the driver and into the footwell. After coughing the droplets emitted from the driver are entrained in the ventilation stream toward the roof of the car and thus more droplets tend to escape the domain. While the current simulation is based on the interior of a Prius, one of the top hybrid electric vehicles sold in the United States of America,[55] and a popular rideshare vehicle interior dimensions of different makes and models of cars and ventilation parameters will affect droplet trajectories and deposition. The interior space in a cabin, the shape of the ceiling, and the location of the outlet influences the flow field and correspondingly affect droplet trajectories and deposition. Additionally, the locations of the vents and ventilation modes and parameters vary between different makes and models of cars. In addition, whether the vehicle is in recirculation mode and is equipped with an interior air filter also impacts the trajectories of aerosolized droplet nuclei. The recirculation mode filters large solid particles but is less effective at filtering particles 0.3 μm, which would result in re-entrainment of the droplet nuclei in the vehicle interior. The complexity of ventilation and interior designs in different makes and models of passenger cars limits the generalizability of the results in terms of the absolute droplet fractions deposited on surfaces within passenger cars. Simulated respiratory particle transmission under different natural ventilation configurations (with different window open locations) in a bus[56] showed that the presence of natural air ventilation circulated viral particles more significantly than removing them from the bus, thus the most efficient ventilation system on a bus to minimize the viral exposure is to keep the window closed. Similarly, fully opening all windows is not always the best choice in an open window passenger car, with one front window and the diagonal rear window open shows the best ventilation efficiency.[57] In such small size passenger cars, the virus generated by front-seated travelers is 5 to 10 times easier to be vented out than the rear-seated travelers.[57] The current simulation used a configuration with windows closed because driving with windows open is rare in Los Angeles, the context of these simulations, as high vehicle speeds induce significant buffeting and road noise effects that impair passenger comfort.[58,59]

Facemask use

Measures that have been implemented in supermarkets and shared-ride vehicles such as facemask use, and implementation of partitions have a significant potential to change droplet nuclei trajectories and deposition patterns. In general, wearing a mask limits the number of larger droplet sizes that escape the mask, reduces the total number of droplets emitted into the indoor air, and reduces droplet velocities by ~40 to 50%.[4,60] Surgical face masks were reported to significantly reduce the detection of influenza virus RNA in respiratory droplets and coronavirus RNA in respiratory droplets from symptomatic individuals.[61] The effectiveness of facemasks in limiting droplet spread in indoor environments, however, is dependent on the materials of the mask,[62] the number of layers,[62] and inward and outward leakage.[63,64] Furthermore, the effectiveness of facemasks in limiting infection is also dependent on handling when contaminated with viral droplets.[65] In the current simulations of supermarket check-out counters and passenger cars, a reduction in the velocity of exhaled droplets combined with the capture of larger droplet sizes eliminates the deposition of larger exhaled droplets in the vicinity of the carrier and proportionally reduces the number of aerosolized droplet nuclei. Wearing of surgical masks or cotton facemasks would reduce emission of residual droplet nuclei (<300 nm) by 76% ± 22, and 79% ± 23, respectively.[66] A reduction in emission of associated viral RNA by ~76%, would correspond to a reduction in maximum concentrations of droplet nuclei deposited on the surfaces down to 197 droplet nuclei/m² and close to zero after coughing and speaking at the supermarket checkout counter, respectively. While the maximum concentrations in the sedan car would be 333 and 4 droplet nuclei/m² after coughing and speaking, respectively.

In conclusion CFD simulations of the dispersion of exhaled droplets in interior spaces on their own, do not represent infection risk as viral RNA is non-linearly distributed across droplet sizes and the links between transmission of virus-laden droplets and infection in individuals are complex due to a range of other virus-host relationships. Incorporation of the non-linear distribution of viral RNA across droplet sizes, however, demonstrates that the larger exhaled droplets that deposit on surfaces have low viral content, which may help explain the apparent importance of inhalation exposures in SARS-CoV-2 transmission, and the lower transmissibility for surface contact observed in the pandemic. The vast majority of exhaled virions in both the supermarket and the passenger car remained entrained in the air until they were ventilated out of the space (approximately 89% and 87% for speaking and coughing respectively in both the supermarket as well as in the passenger car). In both the supermarket and passenger car 0.1% of virions were deposited in the near vicinity of the person and 10.5% to 12% in the remainder of the interior space. Maximum viral RNA on surfaces in the supermarket was 2.3×10^4 virions/m² and maximum surface concentration of 9.3×10^4 virions/m² in the passenger car. Wearing of masks eliminated surface deposition and reduces the viral RNA in residual droplet nuclei which lends additional support to use of facemasks as a preventative measure in communities to reduce transmission.

Acknowledgements

Author Contributions

Conceptualization, E.R., M.P., S.R.N., and Y.H.; Lead Investigator, E.R.; Data fetching, S.R.N. and Y.H.; Formal analysis, S.R.N. and Y.H.; Methodology, S.R.N. and Y.H.; Supervision, M.P.; Writing-original draft, S.R.N., Y.H., and E.R.; Writing-review & editing, E.R. and M.P. All authors have read and agreed to the published version of the manuscript.

Supplemental Material

Supplemental material for this article is available online.

REFERENCES

1. Stelzer-Braid S, Oliver BG, Blazey AJ, et al. Exhalation of respiratory viruses by breathing, coughing, and talking. *J Med Virol*. 2009;81:1674-1679.
2. Prather KA, Wang CC, Schooley RT. Reducing transmission of SARS-CoV-2. *Science*. 2020;368:1422-1424.
3. He Z, Shao S, Li J, Kumar SS, Sokoloff JB, Hong J. Droplet evaporation residue indicating SARS-COV-2 survivability on surfaces. *Phys Fluids*. 2021;33:1-9.
4. Dbouk T, Drikakis D. On respiratory droplets and face masks. *Phys Fluids*. 2020;32:063303.
5. Tellier R, Li Y, Cowling BJ, Tang JW. Recognition of aerosol transmission of infectious agents: a commentary. *BMC Infect Dis*. 2019;19:1-9.
6. Liu Y, Ning Z, Chen Y, et al. Aerodynamic analysis of SARS-CoV-2 in two Wuhan hospitals. *Nature*. 2020;582:557-560.
7. van Doremalen N, Bushmaker T, Morris DH, et al. Aerosol and surface stability of SARS-CoV-2 as compared with SARS-CoV-1. *N Engl J Med*. 2020;382:1564-1567.
8. Yang W, Elankumaran S, Marr LC. Concentrations and size distributions of airborne influenza A viruses measured indoors at a health centre, a day-care centre and on aeroplanes. *J R Soc Interface*. 2011;8:1176-1184.
9. Shao S, Zhou D, He R, et al. Risk assessment of airborne transmission of COVID-19 by asymptomatic individuals under different practical settings. *J Aerosol Sci*. 2021;151:105661.
10. Abuhegazy M, Talaat K, Anderoglu O, Poroseva SV. Numerical investigation of aerosol transport in a classroom with relevance to COVID-19. *Phys Fluids*. 2020;32:103311.
11. Rencken GK, Rutherford EK, Ghanta N, Kongoletos J, Glicksman L. Patterns of SARS-CoV-2 aerosol spread in typical classrooms. *Build Environ*. 2021;204:108167.
12. Li Y, Qian H, Hang J, et al. Probable airborne transmission of SARS-CoV-2 in a poorly ventilated restaurant. *Build Environ*. 2021;196:107788.
13. Dbouk T, Drikakis D. On coughing and airborne droplet transmission to humans. *Phys Fluids*. 2020;32:053310.
14. Li H, Leong FY, Xu G, Ge Z, Kang CW, Lim KH. Dispersion of evaporating cough droplets in tropical outdoor environment. *Phys Fluids*. 2020;32:1-11.
15. Cui F, Geng X, Zervaki O, et al. Transport and fate of virus-laden particles in a supermarket: Recommendations for risk reduction of COVID-19 spreading. *J Environ Eng*. 2021;147:04021007.
16. Standard 62.1-2019 - American Society of Heating, Refrigerating and Air-Conditioning Engineers. Accessed July 15, 2021. https://ashrae.iwrapper.com/ashrae_preview_only_standards/std_62.1_2019.
17. Fojtlín M, Planka M, Fišer J, Pokorný J, Jícha M. Airflow measurement of the car HVAC unit using hot-wire anemometry. *EPJ Web Conf*. 2016;114:1-6.
18. Chao CYH, Wan MP, Morawska L, et al. Characterization of expiration air jets and droplet size distributions immediately at the mouth opening. *J Aerosol Sci*. 2009;40:122-133.
19. Popov TA, Kralimarkova TZ, Labor M, Plavec D. The added value of exhaled breath temperature in respiratory medicine. *J Breath Res*. 2017;11:034001.
20. Liu L, Wei J, Li Y, Ooi A. Evaporation and dispersion of respiratory droplets from coughing. *Indoor Air*. 2017;27:179-190.
21. Bar-On YM, Flamholz A, Phillips R, Milo R. Sars-Cov-2 (Covid-19) by the numbers. *eLife*. 2020;9:1-15.
22. Kim J-M, Chung Y-S, Jo HJ, et al. Identification of coronavirus isolated from a patient in Korea with COVID-19. *Osong Public Heal Res Perspect*. 2020;11:3-7.
23. Brochot C, Bahloul A, Abdolghader P, Haghighat F. Performance of mechanical filters used in general ventilation against nanoparticles. *IOP Conference Series: Materials Science and Engineering*. 2019;609:032044.
24. Wölfel R, Corman VM, Guggemos W, et al. Virological assessment of hospitalized patients with COVID-2019. *Nature*. 2020;581:465-469.
25. Morawska L, Buonanno G. The physics of particle formation and deposition during breathing. *Nat Rev Phys*. 2021;3:300-301.
26. Coleman KK, Tay DJW, Tan KS, et al. Viral load of severe acute respiratory syndrome coronavirus 2 (SARS-CoV-2) in respiratory aerosols emitted by patients with coronavirus disease 2019 (COVID-19) while breathing, talking, and singing. *Clin Infect Dis*. 2022;74:1722-1728.
27. Zhang M, Shrestha P, Liu X, et al. Computational fluid dynamics simulation of SARS-CoV-2 aerosol dispersion inside a grocery store. *Build Environ*. 2022;209:108652.
28. Arpino F, Grossi G, Cortellessa G, et al. Risk of SARS-CoV-2 in a car cabin assessed through 3D CFD simulations. *Indoor Air*. 2022;32:1-20.
29. Saw LH, Leo BF, Nor NSM, et al. Modeling aerosol transmission of SARS-CoV-2 from human-exhaled particles in a hospital ward. *Environ Sci Pollut Res*. 2021;28:53478-53492.
30. Talaat K, Abuhegazy M, Mahfoze OA, Anderoglu O, Poroseva SV. Simulation of aerosol transmission on a Boeing 737 airplane with intervention measures for COVID-19 mitigation. *Phys Fluids*. 2021;33:033312.
31. Faleiros DE, van den Bos W, Botto L, Scarano F. TU Delft COVID-App: a tool to democratize CFD simulations for SARS-CoV-2 infection risk analysis. *Sci Total Environ*. 2022;826:154143.
32. Santarpia JL, Rivera DN, Herrera VL, et al. Author correction: aerosol and surface contamination of SARS-CoV-2 observed in quarantine and isolation care. *Sci Rep*. 2020;10:1-8.
33. Anderson EL, Turnham P, Griffin JR, Clarke CC. Consideration of the aerosol transmission for COVID-19 and public health. *Risk Anal*. 2020;40:902-907.
34. Klompas M, Baker MA, Rhee C. Airborne transmission of SARS-CoV-2: theoretical considerations and available evidence. *JAMA*. 2020;324:441-442.
35. Morawska L, Cao J. Airborne transmission of SARS-CoV-2: the world should Face the reality. *Environ Int*. 2020;139:105730.
36. You SH, Chen SC, Wang CH, Liao CM. Linking contact behavior and droplet patterns to dynamically model indoor respiratory infections among schoolchildren. *J Epidemiol*. 2013;23:251-261.
37. Chaudhuri S, Basu S, Kabi P, Unni VR, Saha A. Modeling the role of respiratory droplets in covid-19 type pandemics. *Phys Fluid*. 2020;32:063309.
38. Santarpia JL, Herrera VL, Rivera DN, et al. The size and culturability of patient-generated SARS-CoV-2 aerosol. *J Expo Sci Environ Epidemiol*. 2022;32:706-711.
39. Lavezzo E, Franchin E, Ciavarella C, et al. Suppression of a SARS-CoV-2 outbreak in the Italian municipality of Vo'. *Nature*. 2020;584:425-429.
40. Rothe C, Schunk M, Sothmann P, et al. Transmission of 2019-NCoV infection from an asymptomatic contact in Germany. *New Engl J Med*. 2020;382:970-971.
41. Buonanno G, Morawska L, Stabile L. Quantitative assessment of the risk of airborne transmission of SARS-CoV-2 infection: prospective and retrospective applications. *Environ Int*. 2020;145:106112.
42. Riediker M, Tsai DH. Estimation of viral aerosol emissions from simulated individuals with asymptomatic to moderate coronavirus disease 2019. *JAMA Netw Open*. 2020;3:e2013807.
43. Wang CC, Prather KA, Sznitman J, et al. Airborne transmission of respiratory viruses. *Science*. 2021;373:80.
44. Johnson GR, Morawska L, Ristovski ZD, et al. Modality of human expired aerosol size distributions. *J Aerosol Sci*. 2011;42:839-851.
45. Wölfel R, Corman VM, Guggemos W, et al. Virological assessment of hospitalized cases of coronavirus disease 2019. *Nature*. 2020;581:465-469.
46. Koster F, Gouveia K, Zhou Y, et al. Exhaled aerosol transmission of pandemic and seasonal H1N1 influenza viruses in the ferret. *PLoS One*. 2012;7:1-14.
47. Sette A, Crotty S. Adaptive immunity to SARS-CoV-2 and COVID-19. *Cell*. 2021;184:861-880.
48. Cao X. COVID-19: Immunopathology and its implications for therapy. *Nat Rev Immunol*. 2020;20:269-270.
49. Ramasamy R. Perspective of the relationship between the susceptibility to initial Sars-Cov-2 infectivity and optimal nasal conditioning of inhaled air. *Int J Mol Sci*. 2021;22:7919.
50. Morozov VN, Mikheev AY. A collection system for dry solid residues from exhaled breath for analysis via atomic force microscopy. *J Breath Res*. 2017;11:016006.
51. Papineni RS, Rosenthal FS. The size distribution of droplets in the exhaled breath of healthy human subjects. *J Aerosol Med Depos Clear Eff Lung*. 1997;10:105-116.

52. Hamner L, Dubbel P, Capron I, et al. High SARS-CoV-2 attack rate following exposure at a choir practice — Skagit County, Washington, March 2020. *Morb Mortal Wkly Rep High*. 2020;69:606-610.

53. Lewis D. Lewis-2021_the superspreading problem _ nature. *Nature*. 2021; 590:544-546.

54. Gładyszewska-Fiedoruk K, Teleszewski TJ. Modeling of humidity in passenger cars equipped with mechanical ventilation. *Energies*. 2020;13:2987.

55. Alternative Fuels Data Center: Maps and Data - U.S. HEV Sales by Model. Accessed September 5, 2021. https://afdc.energy.gov/data/10301.

56. Zafar MU, Lee V, Timms W, Bounds P, Uddin M. Effects of HVAC settings and Windows Open or close on the SARS-COV-2 virus transmission inside A mass transit system bus. *ASME Int Mech Eng Congr Expo Proc*. 2021; 10:1-10.

57. Shu S, Mitchell TE, Wiggins MRR, You S, Thomas H, Li C. How opening windows and other measures decrease virus concentration in a moving car. *Eng Comput*. 2022;39:2350-2366.

58. Wang Q, Chen X, Zhang Y. An overview of automotive wind noise and buffeting active control. *SAE Int J Veh Dyn Stab NVH*. 2021;5:443-458.

59. Dunai L, Lengua I, Iglesias M, Peris-Fajarnés G. Buffeting-noise evaluation in passenger vehicle BMV 530d. *Acoust Phys*. 2019;65:578-582.

60. Kähler CJ, Hain R. Fundamental protective mechanisms of face masks against droplet infections. *Journal of Aerosol Science*. 2020;148:105617.

61. Leung NHL, Chu DKW, Shiu EYC, et al. Respiratory virus shedding in exhaled breath and efficacy of face masks. *Nat Med*. 2020;26:676-680.

62. Asadi S, Cappa CD, Barreda S, Wexler AS, Bouvier NM, Ristenpart WD. Efficacy of masks and face coverings in controlling outward aerosol particle emission from expiratory activities. *Sci Rep*. 2020;10:1-13.

63. Grinshpun SA, Haruta H, Eninger RM, Reponen T, McKay RT, Lee SA. Performance of an N95 filtering facepiece particulate respirator and a surgical mask during human breathing: two pathways for particle penetration. *J Occup Environ Hyg*. 2009;6:593-603.

64. Chiera S, Cristoforetti A, Benedetti L, et al. A simple method to quantify outward leakage of medical face masks and barrier face coverings: implication for the overall filtration efficiency. *Int J Environ Res Public Health*. 2022;19:3548.

65. Chughtai AA, Stelzer-Braid S, Rawlinson W, et al. Contamination by respiratory viruses on outer surface of medical masks used by hospital healthcare workers. *BMC Infect Dis*. 2019;19:1-8.

66. Konda A, Prakash A, Moss GA, Schmoldt M, Grant GD, Guha S. Response to letters to the editor on aerosol filtration efficiency of common fabrics used in respiratory cloth masks: revised and expanded results. *ACS Nano*. 2020;14:6339-6347.